crystals

MDPI

Review

Innovation in Metal Casting Processes: A Review of Metal Matrix Nanocomposites in Metal and Bimetal Castings

Tayyab Subhani [1,*], Mohamed Ramadan [1,2,*], Naglaa Fathy [3], Abdel Khaliq [1] and K. S. Abdel Halim [1,2]

[1] College of Engineering, University of Ha'il, Ha'il P.O. Box 2440, Saudi Arabia; ab.ismail@uoh.edu.sa (A.K.); k.abdulhalem@uoh.edu.sa (K.S.A.H.)
[2] Central Metallurgical Research and Development Institute (CMRDI), P.O. Box 87, Helwan 11421, Egypt
[3] Department of Physics, College of Science, University of Ha'il, Ha'il P.O. Box 2440, Saudi Arabia; n.ismail@uoh.edu.sa
* Correspondence: ta.subhani@uoh.edu.sa (T.S.); m.ramadan@uoh.edu.sa (M.R.)

Abstract: The arrival of nanotechnology in the field of metal castings is considered a promising approach to significantly improve the quality, performance and lifetime of castings. A better understanding of the implementation of nanotechnology in the metal casting process and its dynamics is essential for the successful production of metal matrix nanocomposite castings. This review focuses on past and present techniques for metal matrix nanocomposite castings to facilitate future fabrication processes and improve the performance of casting products. The advantages, limitations, difficulties and optimal processing conditions of nanocomposite castings are presented and thoroughly discussed. Both types of metal matrix nanocomposites (i.e., ferrous and nonferrous metallic matrices, are discussed in the present review), as well as nanocomposites in the working surface layer and interlayer of bimetallic materials. Significant improvements in the surface microstructure and shear strength of bimetallic bearings are achieved using nanoparticles as additions to the surface working layer and interlayer areas. Special emphasis is given to the factors affecting these fabrication processes in achieving high-quality products. The dispersion of nanoparticles in the metallic matrix is another critical issue, which is discussed comprehensively. Moreover, the strengthening mechanisms that evolve due to the incorporation of nanoparticles in the metallic matrices, which deserve separate attention, are discussed. The economic and political factors that simultaneously lead to evolutionary and drastic changes in metal matrix nanocomposite castings are also considered. Finally, the present article indicates future fabrication routes and describes the development of metal matrix nanocomposite castings under the influence of nanotechnology after incorporating the novel casting opportunities presented by nanotechnology.

Keywords: casting; nanotechnology; nanocomposites; nanomaterials; mechanical properties; bimetallic

check for updates

Received: 18 December 2024
Revised: 12 February 2025
Accepted: 13 February 2025
Published: 17 February 2025

Citation: Subhani, T.; Ramadan, M.; Fathy, N.; Khaliq, A.; Halim, K.S.A. Innovation in Metal Casting Processes: A Review of Metal Matrix Nanocomposites in Metal and Bimetal Castings. *Crystals* **2025**, *15*, 191. https://doi.org/10.3390/cryst15020191

Copyright: © 2025 by the authors. Licensee MDPI, Basel, Switzerland. This article is an open access article distributed under the terms and conditions of the Creative Commons Attribution (CC BY) license (https://creativecommons.org/licenses/by/4.0/).

1. Introduction

1.1. Metal Casting Process: History and Facts

There are a variety of manufacturing processes that shape and/or deform metals and their alloys into useful products. The metal casting process is the oldest manufacturing process, which involves melting and pouring a liquid metal into a prefabricated mold. After cooling and solidification, the liquid metal takes the shape of the cavity in the mold. The metal casting process was first used in 4000 B.C. to fabricate arrowheads and numerous other parts and objects. A wide variety of metals have been shaped using the process of

casting. A unique feature of this process is the ability to produce complex shapes containing internal cavities such as engine blocks [1]. Figure 1 shows the image of an engine block fabricated with aluminum alloy [2].

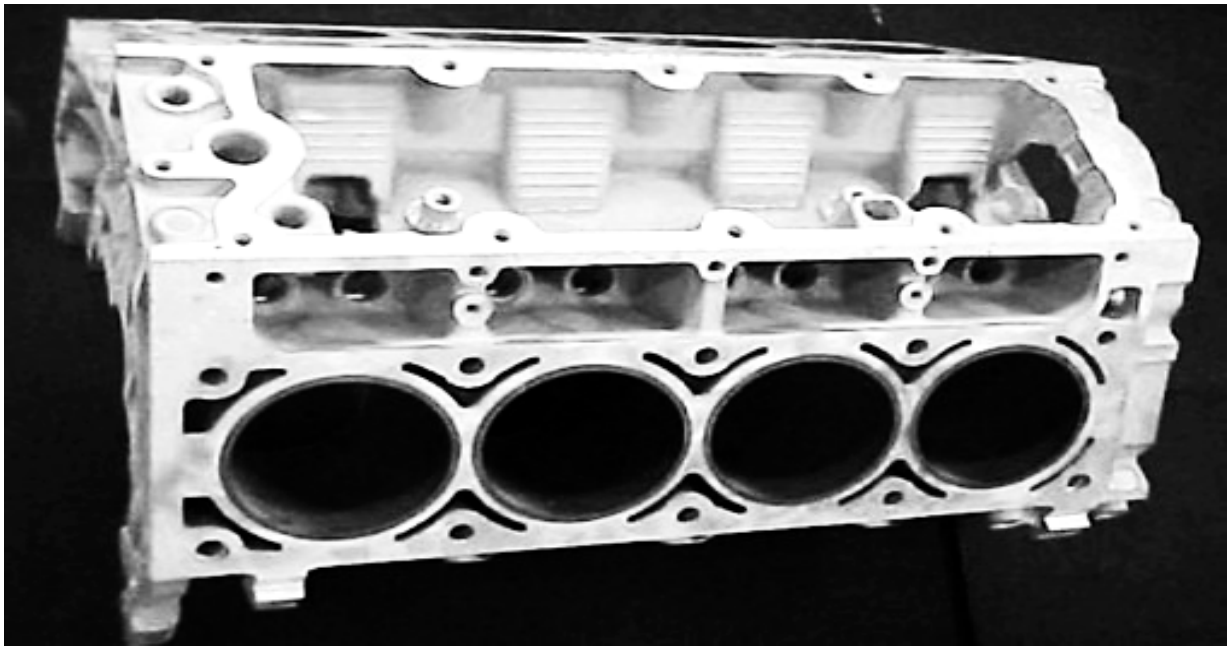


Figure 1. Engine block cast from aluminium alloy [2].

The casting process's unique ability to fabricate large and complex products makes this technique stand out from other manufacturing processes, which are unable to provide as much detail in the final product at a manageable cost. Although the casting process has its own characteristics, costs and advantages, the lower mechanical properties due to solidification behavior without a secondary process and the homogeneity in the microstructure are still issues that need attention and limit the application of casting products requiring exceptionally high-strength loading and a long life span, as well as under severe atmospheric conditions. Despite these limitations, the counteracting advantages have led to tremendous growth in the casting process. Figure 2 shows the development of casting processes over the centuries [3].

(a)

3200 BC	The beginning of the production of castings in Mesopotamia
645 BC	The beginning of sand molding
1776	The use of cupola furnace for the first time in England
1881	Castings were used for the first time in Naval submarine
1897	Investment castings were used
1900	High demand of castings from automotive industry
1907	First patent issued for die casting machine
1941-1945	High demand of castings in World War II
1948	Development of ductile cast iron
2020	44.3 billion dollar sale of United States metal casting

(b)



Figure 2. History of the metal casting process (**a**); pouring liquid metal in mold fabricated by gravity metallic mold casting (**b**).

1.2. Nanotechnology: Definition and History

Nanotechnology refers to those areas in science and engineering where phenomena conducted on atomic or molecular scales are utilized in the design, production and application of materials [4]. Nanotechnology refers to dimensions of less than 100 nm and, especially, with the manipulation of individual atoms and/or molecules [5]. Richard Feynman was the first to highlight and describe the prospects of nanotechnology in the latter half of the twentieth century when he described the possibility of manipulation of materials at the atomic scale [6]. In the last quarter of the twentieth century, the invention of the scanning tunneling microscope made it possible to witness individual atoms, while a few years later, the discovery of Buckminster fullerenes realized the presence of nanomaterials. The following years witnessed the synthesis of nanomaterials for the development of novel materials, which is still in progress. Conventional materials have grain sizes in the micrometer size range, while the reduction in grain size to the nanometer range remarkably improves the properties of materials after tremendously increasing the surface area. Nanomaterials may be in the form of nanoparticles of regular and irregular shape, nanofibers and nanotubes of varying external and internal diameters and nanosheets of variable atomic thicknesses.

The emergence of nanomaterials has influenced every sector of engineering, thus leading to the production of materials for advanced applications. The field of composite materials has also been altered since the arrival of nanotechnology, and a new class of nanocomposites was developed after incorporating nanomaterials into metallic, polymeric and ceramic matrices. In the context of the present review, nanomaterials of different shapes were incorporated in metallic matrices to develop a unique class of metal matrix nanocomposites, offering improved mechanical and functional properties. The intention is always to improve the elastic modulus, as well as tensile and yield strengths at both room and high temperatures, increase the fatigue and creep strengths, and enhance the thermal shock resistance, coefficient of thermal expansion and tribological properties, such as wear resistance and coefficient of friction [7].

Ceramic- and carbon-based nanoreinforcements have always been an attractive choice for metallic matrices for producing nanocomposites. Among ceramic reinforcements, metallic oxides, carbides, nitrides and borides were the immediate choice as nanoreinforcements, including aluminum oxide, silicon dioxide, silicon carbide, boron carbide, titanium carbide, aluminum nitride and titanium diborides. Nanotubes, nanosheets and nanospheres were chosen from the graphitic family of elemental carbon, while nanodiamond particles were selected as nanoreinforcements from the diamond family of elemental carbon. Aluminum has always been the prime choice for the matrix material for metal matrix nanocomposites because of its cost-effectiveness, availability, easy processing and prospects to significantly improve the properties by incorporating nanoreinforcements, while other metallic matrices, including magnesium-, titanium- and iron-based alloys, were also considered [7].

However, the main issue always remains the wettability of the nanoreinforcements in the metallic matrices along with their uniform dispersion, which otherwise results in their agglomeration, thus deteriorating the existing properties of metallic matrices. As a result, scientists and engineers are finding ways and developing a variety of methods to homogeneously disperse nanoreinforcements in metallic matrices to fabricate materials that exhibit an enhanced performance, as discussed further below.

Composite materials have a high probability of enhancing the physical, chemical and mechanical properties of metallic materials, which are superior to conventional metallic materials. With the selection of the type, size and amount of reinforcement, which is the core of a composite design, the enhancement of a target property of a metallic matrix can be controlled [7–9].

The aim of this review is to present, classify and discuss the solidification structure of metal matrix composites (MMCs). Casting involves melting the matrix material, followed by different methods for introducing a reinforcement material into the melt, obtaining suitable dispersions. A greater focus is on a comparison of the different techniques used for solidification of the melt containing suspended dispersoids under selected conditions to achieve the desired distribution of the dispersed phase in the metal and bimetal casting.

2. Nanocomposites in Metal Casting

The present era has seen a focus on manufacturing techniques that produce fabricated materials with superior properties and exhibit better performance and facilitation of the fabrication process. Although intensive development of cast metallic structures and properties has been observed, the possibility of further improving the properties and performance of cast products seems unlikely without the involvement of nanotechnology in the casting process. Nanotechnology can, indeed, open avenues for the production of cast materials with superior properties, especially in areas in which trials have otherwise been practically exhausted. Because of the superior properties of nanocomposite casting, it is increasingly being explored in critical engineering components and structural reinforcements. These materials help improve the physical and mechanical properties of castings, as well as the operational efficiency and longevity, leading to lower maintenance costs and enhanced performance. In addition, the ability to incorporate additional functionalities, such as wear and corrosion resistances, further expands the application potential of these materials in the next generation of engineering materials.

Nanotechnology is considered a promising approach to fabricating products with predetermined functions. Moreover, nanomaterials are also used in cast metals (e.g., cast metal structures with nanocrystalline precipitates) and in molding sand technologies because of their special effects on cast metal properties [10]. It is worth mentioning that all of the casting techniques presented can be applied in the process of casting ferrous and nonferrous metals. However, some difficulties can arise during the process and/or when adding the nanoreinforcement components. The high melting temperatures that are required, along with the need for superheating, as well as the high density of the ferrous metal casting, make some techniques more difficult to apply to ferrous casting and, on the other hand, more suitable for casting nonferrous metals. In the current review, the methods for introducing nanoparticles into ferrous metals are presented first, followed by those for nonferrous metals.

2.1. Methods for Introducing Nanoparticles into Metallic Materials

Despite being traditional materials, iron and steel are still the most widely used metallic materials [11–15]. The advantages of ferrous metals are very explicit, including a low cost and stable performance. Ferrous metals play a significant role in the manufacturing of engineering products [16]. High-strength steel is considered an important metal for the international economy, national security and a key factor of the growth in the engineering industry.

The strengthening mechanisms of ferrous metals include dislocations, phase transformation, grain refinement, second-phase dispersion and solution strengthening [17]. The dispersion of the second phase enhances the strength of ferrous metals but reduces the plasticity, with a simultaneous decrease in the toughness observed. It has been reported [18,19] that both the strength and toughness of ferrous metals can be achieved simultaneously by the refinement of the grains, owing to the effect of the grain refinement together with the pinning of the grain boundaries of small-sized, second-phase particles that restrict the coarsening of the microstructure, which can balance the reduction in toughness. Therefore,

second-phase dispersion and refinement of grains are the most significant methods for strengthening and toughening the ferrous metallic materials [20].

A second phase can either be incorporated or precipitated into the matrix of steel by alloying, a nucleating agent, or particle reinforcement. In this respect, the strengthening effect of the nanoreinforcement is comparatively higher than a micrometer-sized reinforcement. The high surface energy of the nanometer-sized reinforcing agents and changes to the specific gravity of the liquid ferrous metals (i.e., steels and cast irons) and reinforcements make the dispersion of nanometer-sized reinforcements very difficult to achieve [21]. The current review presents the nine most common methods for introducing nanoparticles into ferrous and nonferrous metals. Using nanoparticles as a strengthening or nucleation phase, the lattice mismatch and valence electron between the nanoparticles and the crystal structure of the metal are important criteria for determining the strengthening effect and analyzing the nucleation efficiency.

During the solidification of molten steel at high temperatures, the different carbon contents produce a ferrite or austenite primary phase. Therefore, δ-Fe and/or γ-Fe is expected to be nucleated. The effectiveness of the heterogeneous nucleation and lattice mismatch relationship should be considered during the selection of nanoparticles suitable for the nucleating phase.

Figure 3 presents solidification structures of pure metal, an alloy, and a nucleating agent's structure. The mold walls are much cooler than the liquid metals, resulting in rapid cooling and producing a skin/shell layer, with an equiaxed grain structure called the chill zone. A typical columnar grain structure is subsequently produced after the chill zone. In the microstructure of an alloy, a third type of grain is produced with equal dimensions, called equiaxed grains, which are larger in size than chill zone grains due to the low rate of heat extraction. After the addition of a nucleating agent in the mold, grains of similar size are produced throughout the body of a casting [22].

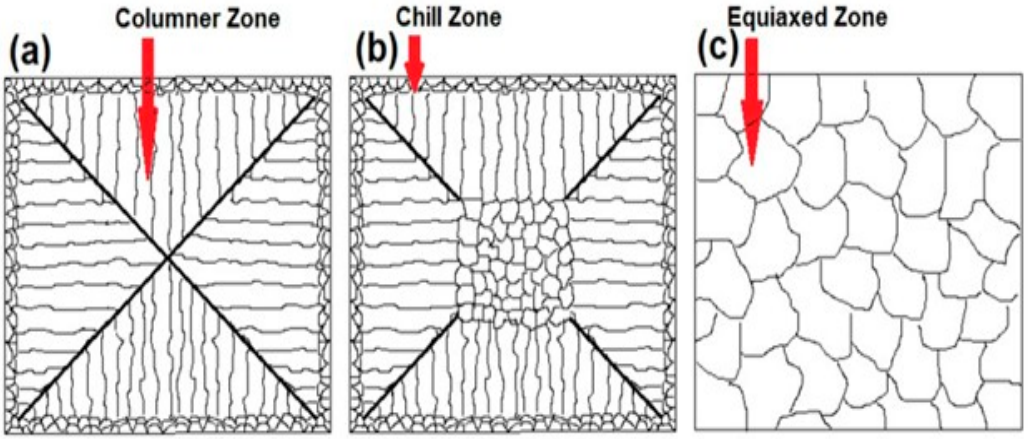


Figure 3. Solidification structure of pure metal (**a**); alloy (**b**); nucleating agent's structure (**c**).

It was reported [23] that greater conducive heterogeneous nucleation can be achieved by a smaller mismatch between the nucleation phase and substrate. Super cooling has a significant effect on the mismatch of both the nucleation phase and substrate. In the case of a less than 12% mismatch (δ), significant heterogeneous nucleation can be achieved. The theoretical method for the dimensional mismatch of the lattice is calculated using the following equation [20]:

$$\delta_{(hkl)n}^{(hkl)_s} = \sum_{i=1}^{3} \frac{\frac{\left|d[uvw]_s^i cos\theta - d[uvw]_n^i\right|}{d[uvw]_n^i}}{3} \times 100\% \quad (1)$$

where (*hkl*)*s* = the low index plane of the substrate; [*uvw*]*s* = the low index direction in (*hkl*)*s*; (*hkl*)*n* is the low-index plane of the nucleated phase; [*uvw*]*n* is the low-index direction in (*hkl*)*n*; *d*[*uvw*]*s* is the interatomic distance along [*uvw*]*s*; *d*[*uvw*]*n* is the interatomic distance along [*uvw*]*n*; and θ is the angle between [*uvw*]*s* and [*uvw*]*n*.

All variables are defined in the literature [23]. Mismatches of popular oxide and carbide with their index crystal planes of γ-iron and δ-iron in the metallurgical steel preparation at a higher temperature of 1500 °C have already been estimated (see Table 1).

Table 1. Compounds' crystallographic parameters and their mismatch with γ-iron and δ-iron [23–25].

Compound	Lattice Type	Lattice Constant (nm)		Mismatch (%)	
		25 °C	1500 °C	δ-Fe	γ-Fe
δ-Fe		-	a = 0.29396	-	-
γ-Fe		-	a = 0.36810	-	-
CaO	Fm3m	a = 0.48105	a = 0.49086	16.51	5.71
Cas	Fm3m	a = 0.56903	a = 0.58158	1.08	11.72
MgO	Fm3m	a = 0.42112	a = 0.43060	3.58	16.98
MgS	Fm3m	a = 0.52033	a = 0.53180	9.54	2.16
MnO	Fm3m	a = 0.44457	a = 0.45517	9.49	12.96
MnS	Fm3m	a = 0.52233	a = 0.53651	8.74	3.06
NbC	Fm3m	a = 0.44702	a = 0.45185	8.69	13.20
NbN	Fm3m	a = 0.43934	a = 0.44474	6.98	14.57
TiC	Fm3m	a = 0.43257	a = 0.43783	5.32	15.89
TiN	Fm3m	a = 0.42419	a = 0.43055	3.57	16.96
TiO	Fm3m	a = 0.41796	a = 0.42624	27.69	15.79
VC	Fm3m	a = 0.41819	a = 0.42271	1.66	14.83
VN	Fm3m	a = 0.41396	a = 0.41907	0.81	13.85
ZrC	Fm3m	a = 0.46961	a = 0.47496	14.25	8.76
ZrN	Fm3m	a = 0.45755	a = 0.46318	11.42	11.02
CeO_2	Fm3m	a = 0.54112	a = 0.55183	6.14	6.00
SiO_2	Fd3m	a = 0.71300	a = 0.71487	14.02	2.90
Ce_2O_3	P-3m1	a = 0.38910, c = 0.60590	a = 0.39704	4.49	14.21
La_2O_3	P-3m1	a = 0.39381, c = 0.61361	a = 0.40184	3.34	13.17
Al_2O_3	P63mc	a = 0.47589, c = 1.29910	a = 0.48224	8.04	7.36
Ti_2O_3	P63mc	-, -	a = 0.51251	6.61	1.55
TiO_2	P42/mnm	a = 0.45937, c = 1.295087	a = 0.46550, c = 0.30080	7.69	8.83
ZrO_2	P42/nmc	-, -	a = 0.36526, c = 0.52969	12.14	0.77

Figure 4 shows the linear relationship between the mismatch and supercooling at a temperature of 1500 °C using an ingot. It can also be observed in Figure 4 that greater conduciveness to heterogeneous nucleation can be achieved by a smaller mismatch (δ).

It is reported that δ-Fe homogeneous nucleation supercooling is 150 °C; otherwise, the supercooling is 50 °C with the use of a substrate of tin or Ce_2O_3 [23–28]. Referring to both of the regressed straight lines in Figure 4, with supercooling of less than 50 °C, the apparent mismatches, δ, of the heterogeneous nucleation are ~8% and ~18%, respectively.

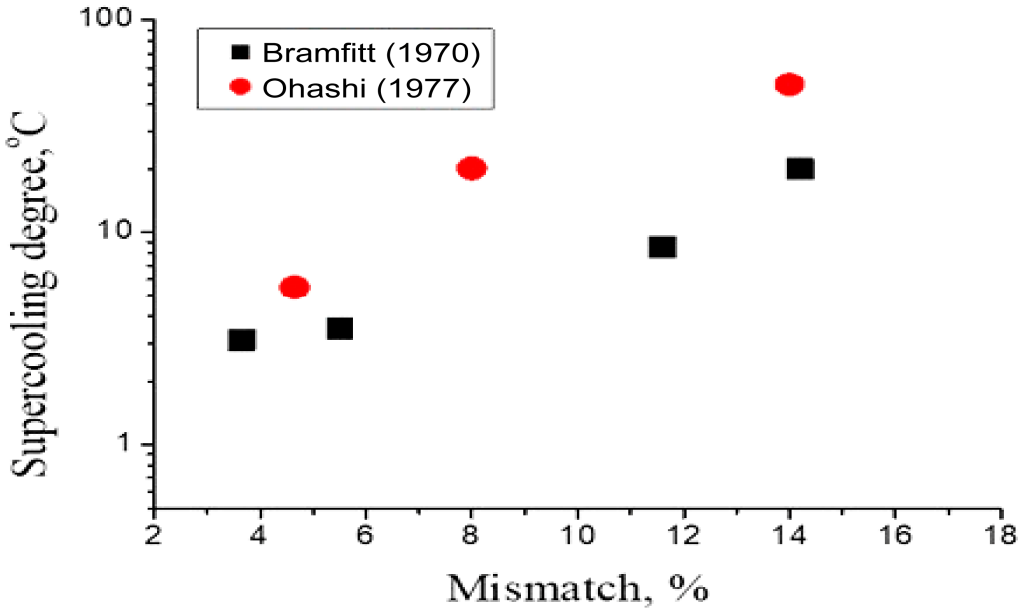


Figure 4. Relationship between the mismatch and supercooling (logarithm) [26,27].

2.1.1. Metal Matrix Composites with External Nanoparticle Addition

The available manufacturing techniques for MMCs are still challenging and relatively expensive. These common casting techniques usually culminate from nanoparticles in addition to a liquid metallic matrix, which is prone to nanoparticle agglomeration and an inhomogeneous matrix microstructure. For example, to prepare nanoparticle-reinforced steel materials, the addition of nanoparticles is considered the simplest manufacturing technique [29–35]. The main problems with using external nanoparticle techniques are the formation of agglomerations due to poor dispersion and their tendency to float on liquid metal because of their greater surface area and difference in densities between the reinforcement and matrix. To avoid such problems in manufacturing, metallic master alloys containing pre-dispersed nanoparticles should be used. Moreover, during hot mixing, the prefabricated nanoparticle master alloys are gradually dispersed and dissolve in the molten matrix.

It was reported [36] that to improve the distribution and uniformity of nanometer-sized NbCs in steel matrix, the addition of Ti to prepare (NbTi)C surface-modified nanoparticles has become obligatory. Both ball milling and mechanical alloying were used with the assistance of a vacuum furnace. After the addition of (NbTi)C particles of ~50–200 nm in size, the ferrite content increased and the colonies of pearlite were separated by ferrite, resulting in refined pearlite with an irregular shape and lamellae-degenerated cementite. Grains of steel sharply decreased to 34 μm and were dramatically refined compared to the size of steel grains in as-cast conditions, which have a value of 184 μm. The mechanical properties of 1045 steel increased after the addition of the abovementioned nanoparticles from 376 to 535 MPa, while the hardness rose from 214 to 277 Hv, thus exhibiting a significant increase.

2.1.2. Heat-Treatment Process for Internal Nanoparticle Formation

Medium- and high-carbon cast steels can be upgraded to high-strength steels by heat treatment because of the formation of internal nanoparticles. The uniform precipitation and dispersion of in situ nanoparticles can be accomplished after optimizing the heat-treatment process, which occurs after alloying and the appearance of deformation-induced precipitates [36–39]. Thus, heat-treatment optimization is the prime route for controlling the distribution and precipitation of nanoparticles. The microstructures of bainitic and/or

martensitic steels are refined by hydrogen diffusion in steel that results in enhancing the resistance to stress corrosion cracks [40].

An ultrafine ferrite phase, together with a homogeneous martensitic distribution, can result in ultra-high strength, along with suitable ductility, in steels, which can be achieved by cold rolling after applying an inter-critical annealing heat treatment. Moreover, low-temperature normalizing can refine the carbides, resulting in high yield strength values [41]. Furthermore, the size and dispersion quality of the precipitates and/or intermetallics also determine the steel's properties and performance.

In one study, nanoparticles were formed in situ in the microstructure of the high-strength low-alloy (HSLA) steel HSLA-100, which improved the mechanical properties because of the strengthening effect of the in situ nanoparticles [42]. The ultimate strength (1047–1103 MPa), yield tensile strength (1008–1068 MPa), and elongation (17–18) of the steel in this study were similar. However, the Charpy V-notch energy (CVN) increased from 32 J to 115 J. Figure 5 shows melted steel in a vacuum furnace with additions of Ti/Al using argon bottom blowing before the last stage casting. It was found that the inclusions in the steel casting showed a core–shell structure of Al_2O_3 with a small content of Ti and an outer shell of MnS, along with a small content of CaS. The other phase was found to be Ti_3O_5 in the matrix, which has a body-centered cubic (BCC) α-iron structure. Moreover, a considerable number of uniformly dispersed nanoparticles were observed.

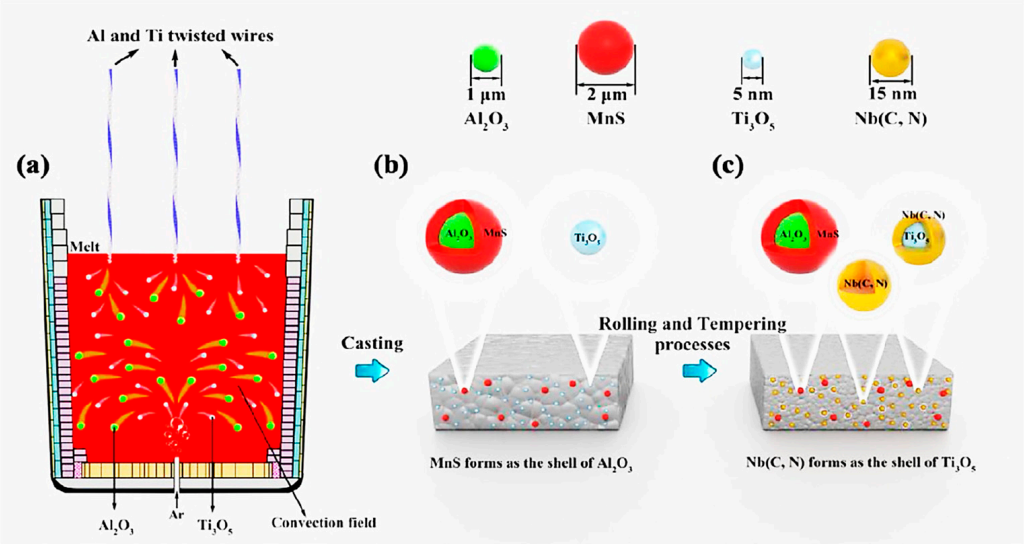


Figure 5. Schematic of the (**a**) element regional supply technique along with (**b**) casting and (**c**) tempering [42].

Nanoparticle-reinforced steel composites can be fabricated with the assistance of an alloying element, along with suitable subsequent plastic deformation and heat-treatment processes. With this manufacturing route, a remarkable improvement in the microstructure and strength can be achieved. Alternatively, high-cost alloying element additions are required to achieve the equivalent results.

The importance of rare earth elements in the purification of the molten steel cannot be neglected, which improves the mechanical properties of steel because of the formation of oxide nanoparticles during the purification process [43,44]. For ferritic/martensitic steel with 9% Cr, the creep strength was improved by the addition of yttrium. Although the initial creep rates of steel with and without the addition of yttrium are almost the same, the creep life of steel with 0.3% yttrium lasted about 2–3 times longer than steel without yttrium. The formation of nanometer-sized oxide clusters during creep is due to the local segregation and diffusion of dissolved oxygen and yttrium atoms at high temperature.

2.1.3. In Situ Nanosized Particle Formation

The idea of utilizing impurity elements in steelmaking to form nanoparticles and, thus, strengthen the steel has attained considerable respect. Currently, nanometer-sized oxide dispersion-strengthened (ODS) cast steels are considered the most promising metallic metals [44–46]. The uniform dispersion of stable nanometer-sized oxides can prevent dislocation movement and, in some cases, provide a pinning effect on grain boundaries. Because of the presence of fine precipitated particles, dislocations are prevented from moving which, in turn, helps greatly in raising and improving the ductility and strength of castings simultaneously.

It was reported [47] that the addition of Zr in Fe-Cr-W-Ti-Al-Zr-0.5Y_2O3 improves the oxide particle dispersion and inhibits the formation of YAlO. The stress corrosion crack resistance was significantly improved due to the coherent and/or semi-coherent relationships of $Y_2Zr_2O_7$ and $Y4Zr_3O_{12}$ with the steel matrix.

2.1.4. Selective Laser Melting for Steel Nanocomposite Manufacturing

The conventional manufacturing of steel nanocomposite castings includes dispersion and melting. A poor interface and an inhomogeneous dispersion of reinforcements are usually observed to lower the physicochemical properties. Additive manufacturing (AM) or three-dimensional (3D) printing has been extensively used in the fabrication of nanoparticle-reinforced steels to overcome these challenges [47–50]. Through data processing and computer-aided design, layer-by-layer stacking of metallic powder has become a novel fabrication technique for complex components. It is non-equilibrium solidification for metals reinforced by high contents of ceramic nanoparticles. Selective laser melting (SLM) (see Figure 6) is the most used additive manufacturing techniques, and it achieves rapid solidification using localized melting by high-density laser beam [51–53].

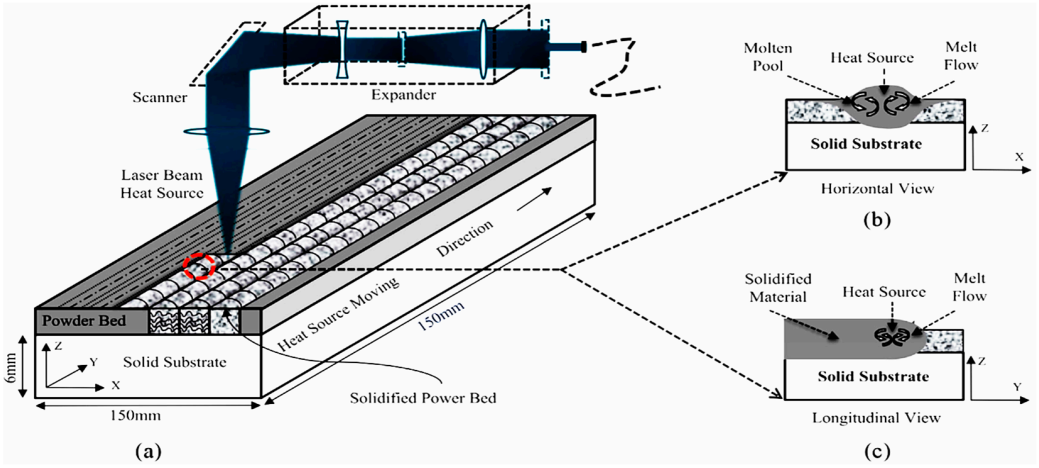


Figure 6. Schematic of the experimental process for SLM (**a**); horizontal view of the domain cross-section (**b**); longitudinal view of the domain cross-section (**c**) [48].

Additive manufacturing is also suitable for manufacturing porous steels that are not suitable for hardcore engineering applications. After novel improvements, AM can be used to fabricate precise and high-quality final parts [51–53].

Heterogeneous nucleation is mainly associated with the interface energy between both the substrate and the nucleated phase. Heterogeneous nucleation can be performed by lowering the interfacial energy, which is highly related to the lattice mismatch (δ), as well as electrostatic potential difference.

Figure 7 shows the solidification of the steel, where small-sized second-phase particles are employed as heterogeneous nucleation sites for the primary crystalline phase,

improving the nucleation process. If not, nanoparticles not involved in the nucleation will be constrained in the dendrites and absorbed at the solid–liquid interface, hindering the dendritic progress and refining the solidification microstructure [54].

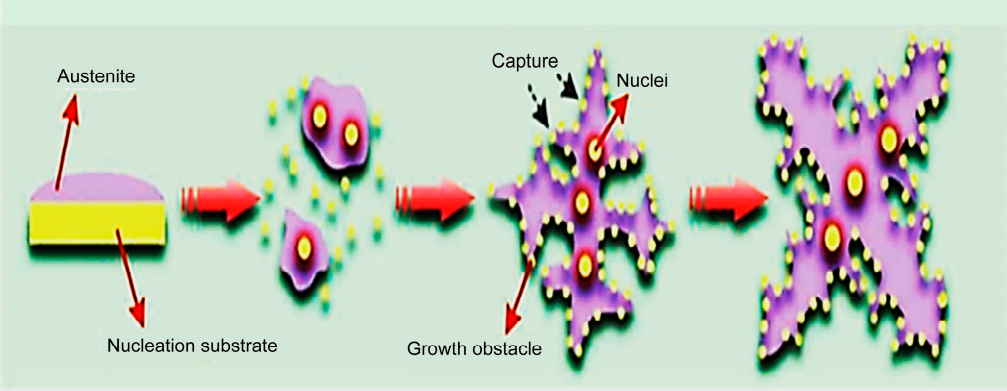


Figure 7. Interaction between the dendritic growth and nanoparticles during the solidification [54].

With the advent of nanotechnology, researchers have developed novel casting techniques to effectively utilize nanometer-sized materials as reinforcement in metallic matrices [55–58]. The common nanometer-sized particles used during these investigations were Ni, Mg, Cu, Al and Ti. Although many of these investigations had disappointing results and did not improve the properties of the metallic matrices, a few were successful and led to significant improvements after the addition of nanometer-sized materials in the metallic matrices. As a result, nanometer-sized carbides, borides, oxides and nitrides are now being used as reinforcements in metal matrix composites to improve the mechanical properties. Furthermore, carbon-based reinforcements are another class of reinforcements that are widely incorporated into metal matrix composites [57].

A range of mechanical properties, including tensile, compressive, ductility, elongation, creep, wear resistance, damping, and dry/wet corrosion resistances, was significantly enhanced by the incorporation of nanometer-scale reinforcing agents in the metallic matrix. Special emphasis was given to lightweight metallic matrices, such as Al and Mg, to improve their mechanical properties after reinforcing with nanoscale materials. However, on an industrial scale, where mass production of composites is needed, many casting techniques that use nanomaterials have not yielded considerable results. One promising solution to avoid these difficulties is to disperse the nanoreinforcements in liquid metal by applying stirring techniques to promote vortex formation [58]. In addition, an alternative technique for the dispersion of nanosized materials in the metal composite formation is the utilization of an ultrasonic system [59–61]. Both stirring and ultrasonic techniques aid in overcoming the problem of the formation nanosized particulate clusters during the fabrication of composites with metallic matrices.

2.1.5. Stir Casting

Stir casting is the simplest procedure for producing MMCs, which depends upon the application of a mechanical stirrer that can be inserted into the liquid metal, which provides homogeneous dispersion of the particles in the metallic matrix. Many ceramic materials have been dispersed in magnesium and aluminum matrices to produce their composites [62,63].

There are three main challenges in the application of the stir-casting technique during the manufacturing of MMCs, as follows: (a) the affinity of nanosized particles to form clusters; (b) the low wettability of nanosized particles with the liquid; and (c) the high porosity in the cast product owing to the entrapment or retention of air due to the stirring

process [64]. As shown in Figure 8, it was reported [65] that the stir casting of Al powder and SiC particulates with sizes in the range of 20–50 nm successfully produced composites by avoiding the abovementioned manufacturing problems.

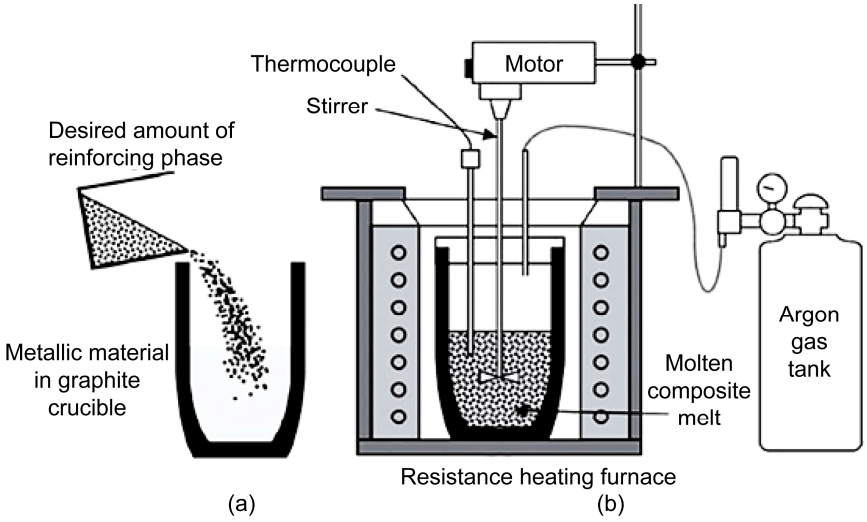


Figure 8. Setup for the stir-casting technique (**a**) addition the reinforcing phase; stir casting process (**b**) [66].

In another investigation [67], the authors studied the microstructural modifications and mechanical characteristics of Al-alloy A356 containing SiC nanoparticles. The alloy was prepared by stir casting at 550 rpm for 10 min and pouring at 680 °C. The results revealed a rise in the yield strength approaching ~41% and in the tensile strength of around ~45%.

2.1.6. Ultrasonic Processing

Ultrasonic processing is an effective manufacturing technique for MMCs. In one study, the mechanical properties of the magnesium-based nanocomposite AZ31/Al_2O_3 were investigated. It was synthesized using an ultrasound-assisted stir-casting technique [68]. Alumina nanoparticles with different weight fractions (0.2–0.5 wt%) were incorporated to produce nanocomposites. During the manufacturing process, the melt was subjected to ultrasonic treatment under controlled temperature conditions. The ultrasound treatment was performed isothermally during air-cooling outside of the furnace (see Figure 9). The grain refinement can be explained in terms of the better heterogeneous nucleation because of the incorporation of the reinforced particles. It was found that the reinforcing agent, which was dispersed by ultrasound technology, greatly enhanced the mechanical properties of the synthesized composites (Figure 10). The manufacturing techniques that used ultrasonic technology show that the coefficient of thermal expansion and Orowan strengthening mechanism were the two main factors improving the strength and behavior of the fabricated composites.

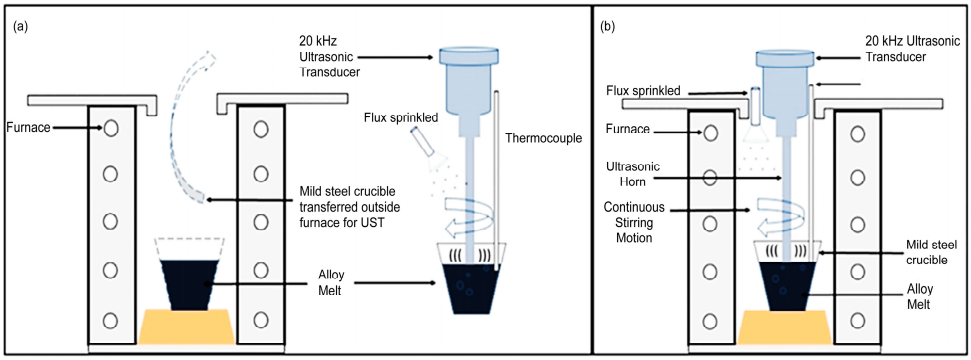


Figure 9. Ultrasonic processing of nanocomposites showing the stirring conducted outside (**a**) and inside the furnace (**b**) [68].

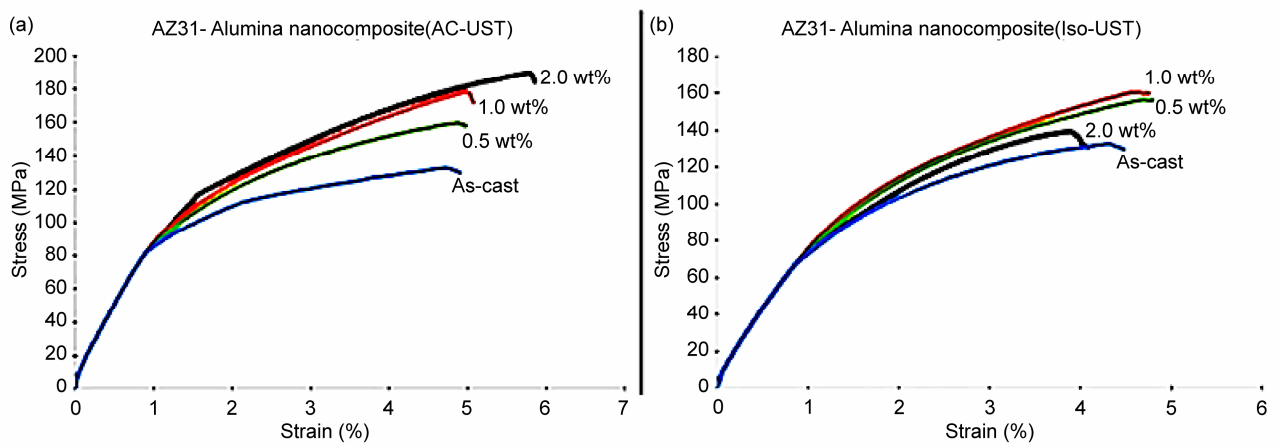


Figure 10. Stress–strain curves of AZ31 alloy and AC-UST samples (**a**) and AZ31 alloy and Iso-UST specimens (**b**) [68].

2.1.7. Disintegrated Melt Deposition Process

The disintegrated melt deposition process is another promising technique used for the fabrication of nanocomposites, which depends mainly on the deposition process and is derived from stir casting [69]. In a study using disintegrated melt deposition, Mg-based nanocomposites were fabricated. A composite slurry was first formed using stir casting, which was passed through a nozzle under an inert gas atmosphere at a superheated temperature. Finally, the slurry was deposited on a metallic substrate. Subsequently, the solidified composite in the form of an ingot was hot extruded to achieve desired shape (Figure 11). Such a process is usually used to produce Mg nanocomposites containing SiC, B_4C, ZrO_2, CNTs, Al_2O_3 and ZnO nanoparticles.

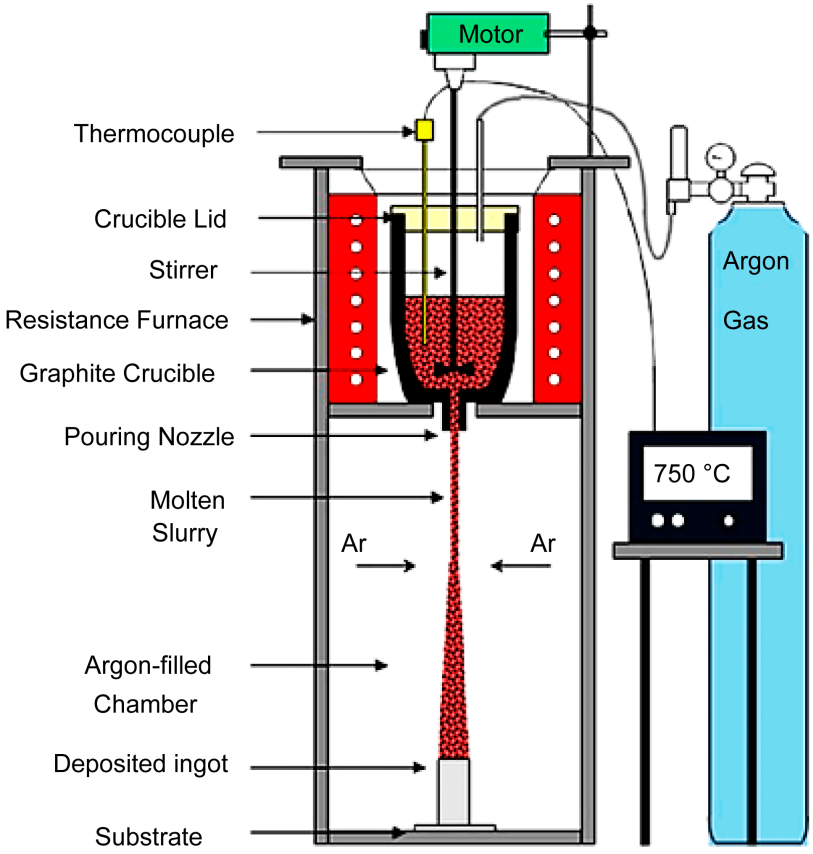


Figure 11. Setup for the disintegrated melt deposition technique [70].

2.1.8. Semi-Solid Casting

In semi-solid casting (SSC), metallic material is forced into a mold cavity in a semi-liquid/solid condition, thus requiring lower energy demands and low porosity, which is conveniently handled, and demands machining after molding than metal casting using other techniques, such as those involving high pressure, including die casting. In general, the method is simple and easily handled, and many metallic alloys have been fabricated using SSC.

In one study [71], nanocomposites containing zinc alloy (AC43A) and 0.5 wt% SiC nanoparticles were cast with 30% fraction of solid material. The produced composite showed significant enhancements in strength with low shrinkage, advancing mold filling and high ductility when compared with liquid-cast AC43A zinc alloy and liquid-cast AC43A/SiC nanocomposites (Figure 12). AM60/SiC nanocomposites were also manufactured using the SSC technique, which had a uniform microstructure.

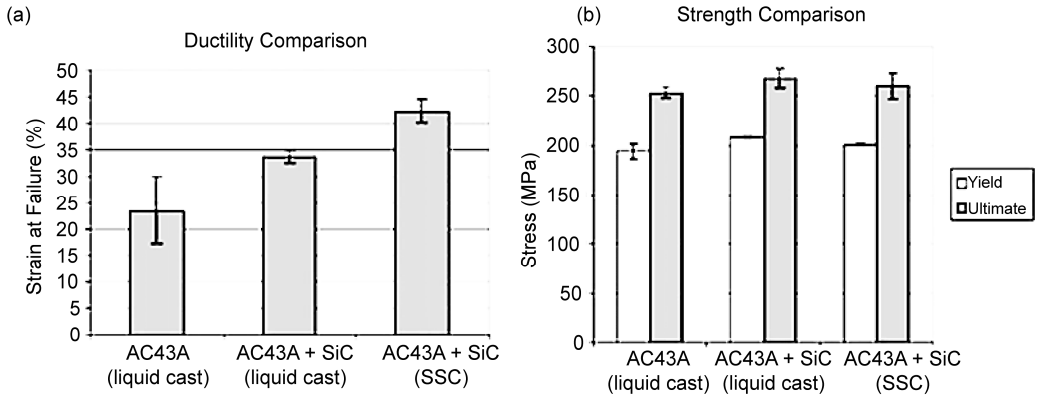


Figure 12. Mechanical properties of liquid AC43A cast alloy without and with the SiC nanocomposite [71].

2.1.9. Dispersion Process

The most challenging aspect in the manufacturing of metal matrix composites is the attainment of an excellent dispersion quality of ceramic nanoparticles in the metallic matrix. The nanoparticles have an obvious inclination toward agglomeration and clustering, owing to their high surface area, which develops van der Waals forces between nanoparticles. As a result, the de-agglomeration of such nanoparticle clusters has become an important task for achieving a metal matrix with a homogeneous nanoparticle distribution. Hereafter, dispersion phenomena of nanoparticles and their mechanisms especially focus on the solidification of composites, ultrasonic cavitation and related phenomena [71–73].

Atoms or molecules of liquid may rupture and form cavities and bubbles after the liquid undergoes a large force or rapid change in pressure. Such a phenomenon is termed as "cavitation inception" [74]. Usually, the force/pressure causing the formation of cavities in the liquid is below the saturated vapor pressure. During proper pressure change, the cavitation bubbles may oscillate in size or shape due to the variation in energy input. At relatively higher pressures, the cavitation bubbles may burst producing severe shock waves in their surrounding environment, producing inertial or transient cavitation.

Although the presence of nanoceramic particles with low density is an important requirement to control the density of the composite, a mandatory mechanical compatibility always exists, which is observed in the small difference in the coefficient of thermal expansion. However, the chemical compatibility of nanoparticles is essential to avoid the particles' dissolution in the melt. However, it is necessary to produce a desirable adhesion to the matrix. Moreover, the melting point of the nanoparticles should be more than that of the matrix, which is the normal situation for ceramic particles. The high modulus of elasticity and high strength that results in good wettability for metallurgical processing are factors

that should be considered. However, one of the most important factors determining the best choice of nanoceramic particles as a reinforcing component in metal matrix composites is the cost of the nanoparticles, which should be inexpensive and economical to prepare.

Many techniques for dispersing nanoparticles and preventing the agglomeration of nanoparticles have been developed. One very efficient approach to uniformly dispersing nanoparticles in molten metal is liquid metal processing supported by external ultrasound. Usually, such manufacturing is followed by a suitable solidification, such as a slow cooling rate. This enables the formation of nanocomposites with a good homogeneous microstructure, and thus the optimal enhancement of the mechanical characteristics of the nanocomposite can be achieved [75,76].

The elementary mechanisms of using ultrasonic techniques in breaking the agglomeration of nanoparticle clusters in molten materials have been investigated extensively by many researchers, both experimentally and by modeling. In summary, there are two main postulations for the deagglomeration mechanisms of nanoparticles, as follows: (a) the high intensity ultrasonic waves produce strong cavitation and (b) the acoustic streaming influences in the liquid metal. In the first mechanism, clustered nanoparticles can be broken via transient cavitation that produces an implosive impact, which is strong enough to break up and disperse the nanoparticles uniformly in the liquid metal (Figure 13a) [77].

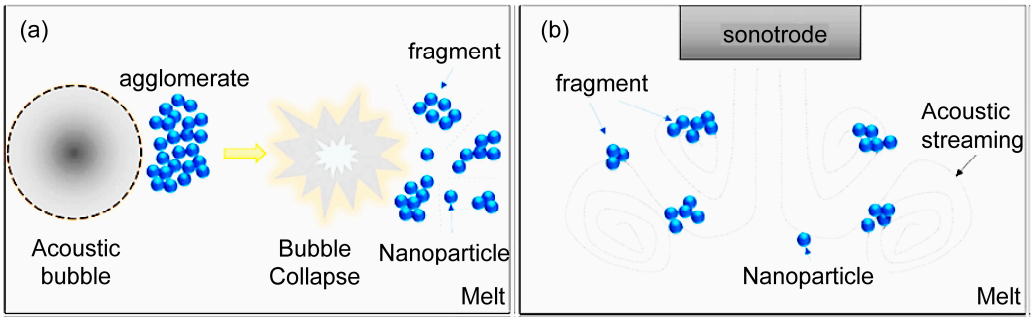


Figure 13. Ultrasonic nanoparticle clusters' deagglomeration for the collapse of the cavitation (**a**); bubble and acoustic streaming (**b**) [77].

It has been observed that the implosive impact can produce pressure in the aluminum melt, which depends on the nearness of the collapsing bubble to the nanoparticle cluster, from 1 MPa to 4 GPa, with an average range of 10~400 MPa [77]. On the other hand, the acoustic streaming in which the liquid flows due to an acoustic pressure change is taken to be very efficient, particularly while stirring, which contributes to the dispersion process (see Figure 13b).

However, no such scenario exists for in situ imaging of the cluster-breaking process for nanoparticles in liquid materials during the ultrasonic cavitation process. Based on a previous study [75], the critical radius of a cavitation bubble in liquid aluminum is around 65 μm under high acoustic pressure.

However, the question arises as to which types of nanoparticles are suitable for reinforcement in metal matrix composites. Usually nanoparticles of carbides, nitrides, oxides and borides are used to reinforce metallic materials [77]. These materials are usually fabricated for industry use at low cost. Table 2 shows the properties of some reinforcement nanoparticles. The usage of ceramic nanoparticles in the metal matrix leads to significant improvements in the characteristics; however, a perfect combination of reinforcement and matrix is required to develop composites with improved properties. Generally, a low density along with increased strength is required along with other related properties.

Table 2. Properties of some reinforcement nanoparticles [77].

Type	SiC	AlN	Al_2O_3	B_4C	TiB_2	TiC
Crystal structure	ac hdp	hdp	ac hdp	rhomb	hdp	cub
Lattice parameters [nm]	a = 0.307, c = 1.008	a = 0.311, c = 0.498	a = 0.476, c = 1.299	a = 0.559, c = 1.205	a = 0.303, c = 0.322	a = 0.432
Melting T [°C]	2300	3000	2045	2450	2900	3140
Young's modulus [GPa]	480	350	410	450	370	320
Density [g/cm^3]	3.22	3.26	3.98	2.53	4.49	4.92
Mohs hardness	9.6	-	6.5	9.5	-	-
CTE [10^{-6} K^{-1}]	4.9	6.0	8.3	5.4	7.4	7.4

3. Strengthening Mechanisms

It is interesting to determine the extent of the improvements in the mechanical properties after the incorporation of nanoparticles in metallic composites. The advantages that ceramic nanoparticles offer for the yield strength of the composites come from various strengthening mechanisms that trigger to varying degrees, depending upon the nature of the reinforcement and matrix, kinds of primary and secondary manufacturing techniques, including mechanical processing or heat treatment. As shown in Equations (2) and (3), the increase in strength can be summed up or the root of the sum of the squares can be taken as the overall influence, respectively. When the effects are independent of each other, the summation method is used. The root of the sum of the square equation is used when the single influences do not act independently, which is the case for large particles.

$\Delta\sigma_{Total}$ is the total increase in the yield strength, while $\Delta\sigma_{GR}$, $\Delta\sigma_{OR}$, $\Delta\sigma_{CTE}$, $\Delta\sigma_{Mod}$ and $\Delta\sigma_{Load}$ are the increase in the yield strength caused by grain refinement, Orowan contribution to the increase in the yield strength, the increase in the yield strength due to the generation of geometrically necessary dislocations during cooling due to the mismatch of the coefficient of thermal expansion of the particles and metal matrix, the input-to-yield-strength increase due to the generation of dislocations created during deformation because of the different elastic moduli in a deformation after casting, and the input-to-yield-strength increase due to the simple presence of reinforcement particles with higher strength, being well-bonded to the immediate matrix [78].

$$\Delta\sigma_{Total} = \Delta\sigma_{GR} + \Delta\sigma_{OR} + \Delta\sigma_{CTE} + \Delta\sigma_{Mod+}\Delta\sigma_{Load} \quad (2)$$

$$\Delta\sigma_{Total=}\sqrt{\Delta\sigma_{GR}{}^2+\Delta\sigma_{OR}{}^2+\Delta\sigma_{CTE}{}^2+\Delta\sigma_{Mod}{}^2+\Delta\sigma_{Load}{}^2} \quad (3)$$

3.1. Orowan Strengthening Mechanism

The Orowan strengthening mechanism is primarily related to strong and hard particles that are dispersed uniformly in the matrix. As a matter of fact, the hard particles restrict the movement of dislocations on their slip planes through the matrix. This influence can be ignored for particles with a diameter >1 μm [79]. Upon the interaction of dislocations with a particle, the dislocations bend around the particle. Subsequently, the dislocations rejoin with themselves and establish a dislocation loop around the particle that results in the improvement of strength. The dislocation then propagates through the matrix. Equation (4) shows the contribution to the strength increase by Orowan strengthening, while Equation (5) shows the geometric description of the interparticle distance [79].

$$\Delta\sigma_{OR} = \frac{0.13bG_m}{\lambda} ln\frac{d_p}{2b} \quad (4)$$

$$\lambda = d_p \left[\left(\frac{1}{2V_p} \right)^{\frac{1}{3}} - 1 \right] \quad (5)$$

where b is the burgers vector; Gm is the shear modulus; d_p is the average diameter of the nanoparticles; and V_p is the volume fraction of the nanoparticles.

3.2. Hall–Petch Strengthening Mechanism

Particles are added during the solidification of metal matrix composites. In manufacturing magnesium alloys, the zirconium element is used for grain refinement. The increase in yield strength is shown by Equation (6), which is called the Hall–Petch equation [78]

$$\sigma_y = \sigma_0 + k_y D^{-\frac{1}{2}} \quad (6)$$

Equation (7) is used to estimate the increase in the yield strength based on the grain refinement achieved by the nanoparticles [75].

$$\Delta\sigma_{GR} = K_y \left(\left(\frac{1}{\sqrt{D_{MMNC}}} \right) - \frac{1}{\sqrt{D_0}} \right) \quad (7)$$

A common example clearly shows the mechanism in the manufacturing of AM60 alloy, which is used in the automotive industry. Figure 14 shows the microstructure of AM60 with and without the addition of AlN [79], which was developed using the ultrasound-assisted casting process. After the addition of nanoparticles, the melt was stirred and subsequently ultrasonicated at a frequency of 20 kHz. A change in the dimensions of grain from 1277.0 ± 301.3 µm to 84.9 ± 6.2 µm augments the yield strength (~103%) and tensile strength (115%) (see Table 3), while the ductility simultaneously increases from 6.4 to 15.4% (~140%).

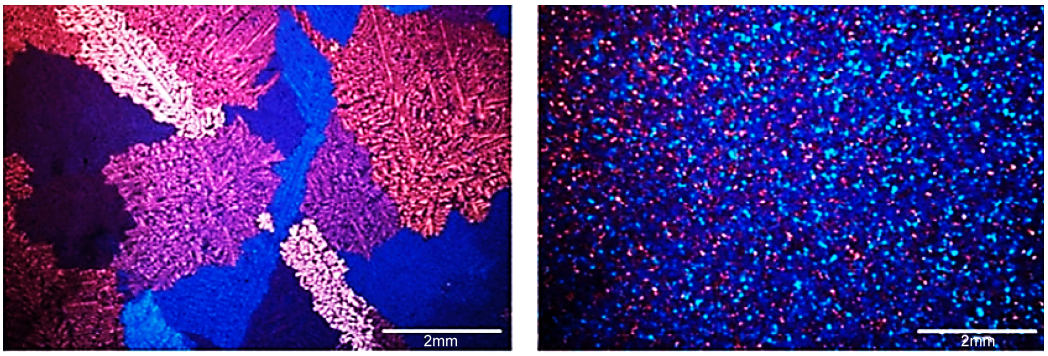


Figure 14. Microstructure of AM60 with (**a**) and without (**b**) the addition of AlN [79].

Table 3. AM60-reinforced properties with an AlN reinforcing agent [75].

Property	AM60	AM60 + AIN
Grain size [µm]	1277.0 ± 301.3	84 ± 6.2
Hardness [HV5]	48.0 ± 4.0	46.4 ± 6.0
Density [g/cm^3]	1.7848 ± 0.0004	1.783 ± 0
Porosity [%]	-	0.919
Yield strength [MPa]	44.9 ± 6.9	91.2 ± 3.8
UTS [MPa]	109.3 ± 19.2	235.1 ± 6.4
Elongation [%]	6.4 ± 3.4	15.4 ± 4.2

One of our achievements in the field of casting metallic composites containing nanoparticles using nanomaterials is the development of an in-house stir-casting process for the manufacturing of hypereutectic Al-Si/graphene nanocomposites with refined and well-distributed primary Si phases [80]. The factors influencing the morphology and hardness of the prepared alloy were investigated. The impacts of cast stirring and graphene nanosheets' (GNSs) incorporation on the microstructural changes and mechanical properties of 393 Al-Si alloys were investigated. A ~17% reduction in the average primary silicon size was acquired with the addition of 1 wt. % GNSs. An outstanding rise in the hardness of the manufactured nanocomposites in comparison to the cast alloy was observed when GNSs were embedded in the Al-Si alloy matrix (Figures 15 and 16).

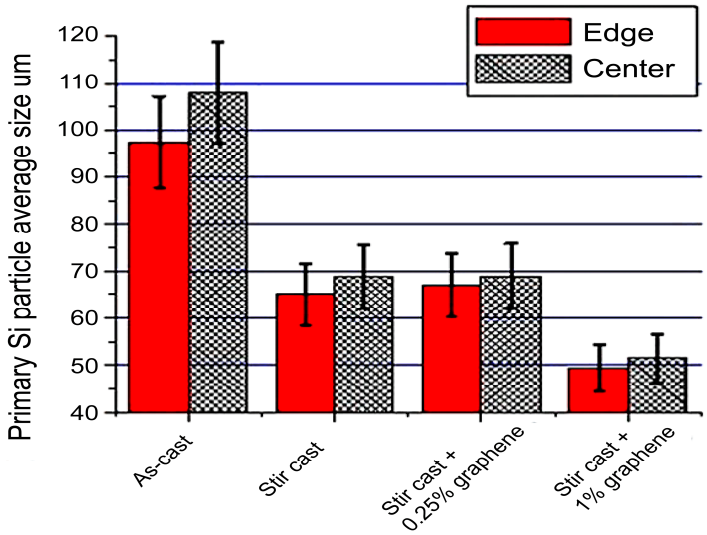


Figure 15. Primary Si particle size with graphene additions [80].

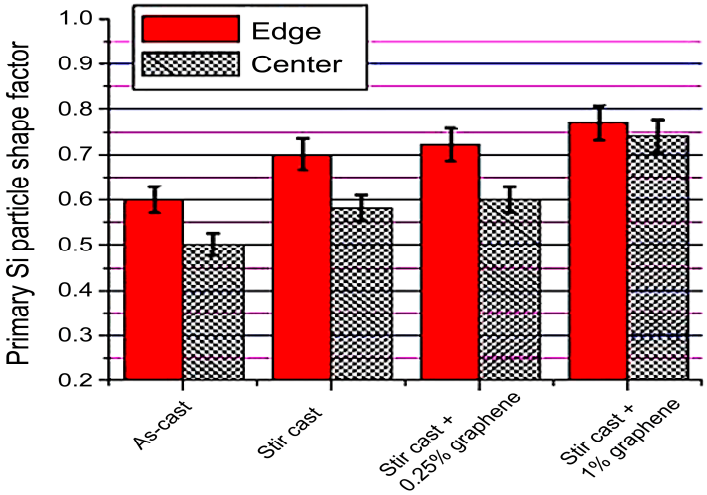


Figure 16. Primary Si SF with graphene nanosheets affects [80].

4. Nanocomposites in Bimetal Casting

Bimetallic materials that are fabricated using metal casting route are divided into the following two main categories: liquid–liquid casting and liquid–solid casting. In liquid–liquid casting, two pouring systems are used to pour the first liquid metal and the second liquid metal respectively [81–83]. In liquid–solid casting, the liquid of the first metal is poured into the mold coating the solid layer of the second metal. The most metallic materials fabricated using bimetal casting are Al, Mg, Cu and Sn alloys as a liquid partner that is poured onto steel, cast iron and copper solid substrates [84–100]. Stir casting is

the most common and commercial casting technique used for nanocomposites bimetallic materials. There is very little research conducted with this approach for ex situ additions of nanoparticles to improve the properties of the surface layer or the interfacial layer of bimetallic materials. Nano ilmenite, alumina silica and iron oxide nanoparticles have been added to Sn-based alloys resulting in significant improvements to the structure and hardness and wear resistances of surface working layers [101–103]

4.1. Nanocomposites in the Working Surface Layer of Bimetallic Materials

Ilmenite ($FeTiO_3$) nanoparticles-reinforced tin Babbitt alloys were successfully fabricated via the stir-casting route with an ultrasonic assist [101]. The work is aimed at improving the mechanical properties of tin Babbitt alloy and optimizing its fabrication processing parameters. The tensile strength of the tin Babbitt alloys improved from 77 MPa to 125.6 MPa with the addition of ilmenite ($FeTiO_3$) nanoparticles.

Sn-based Babbitt alloy doped with alumina nanoparticles was fabricated via the stir-casting technique [86]. The prepared nanocomposite was bonded with a carbon steel substrate to prepare a bimetallic material using stir-casting process (Figure 17). The effect of adding ceramic nanoparticles on the microstructural and mechanical properties was investigated.

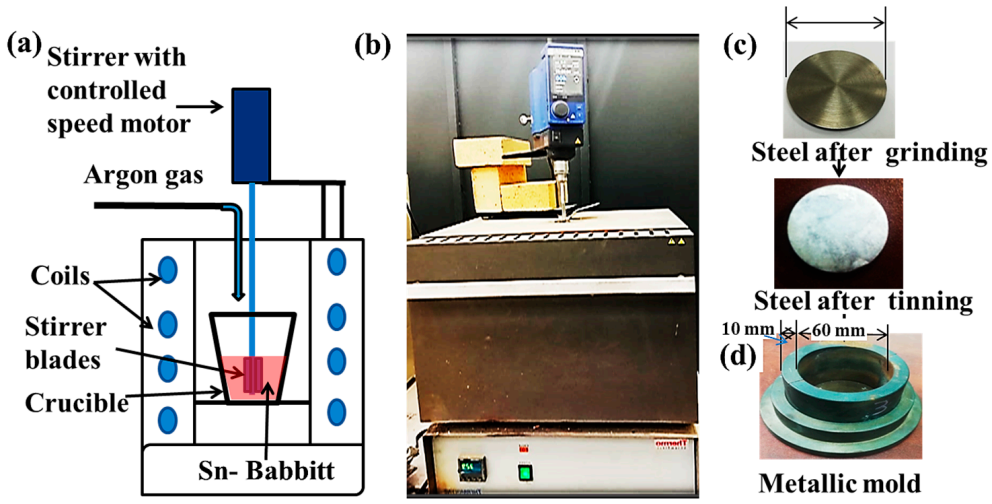


Figure 17. (**a**) Mold and (**b**) furnace employed for manufacturing nanocomposites containing tin-based Babbitt alloy while (**c**) steel after grinding and tinning, and (**d**) mold are also shown. [86].

The nanocomposite was prepared using different loadings of alumina nanoparticles from 0.25 wt% to 1.0 wt%. It was reported that the incorporation of a low fraction of nanoparticles up to 0.50 wt% significantly influenced the morphology and dispersion of Cu_6Sn_5 in the hard phase in a solid solution, leading to needle- and asterisk-shaped modifications to the spherical morphology [102]. The nanocomposites containing up to 0.50 wt% nanoparticles exhibited increases in the tensile strength and better interfacial bonding, and a substantial decline in weight loss was noted during tribological tests with the addition of 0.5 wt% nanoparticles.

Novel nanocomposites of tin-based Babbitt alloy matrix were produced by incorporating iron oxide and silica nanoparticles [102]. The morphology of the Cu_6Sn_5 precipitates changed from an elongated to a spherical shape in the microstructures after the addition of the nanoparticles (Figure 18). The dual effects of the incorporation of the two types of nanoparticles led to a significant increase in the output of ~7.9%. The dual addition of 0.25 wt% iron oxide and 0.25 wt% silica nanoparticles improved the mechanical properties, such as hardness, compressive strength, and wear and friction.

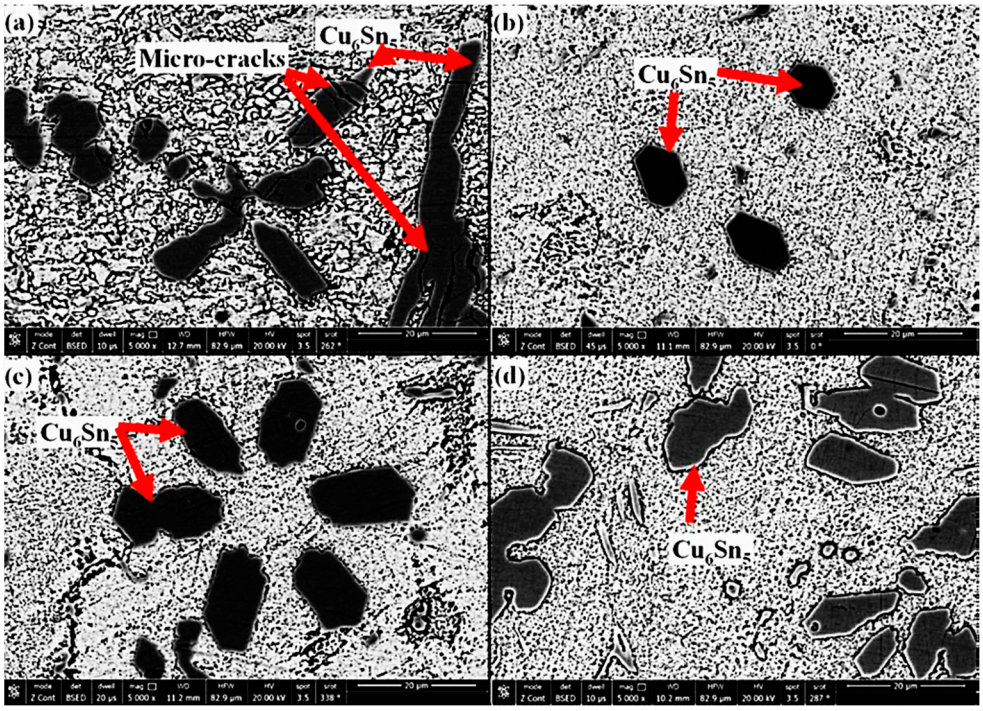


Figure 18. SEM images showing the morphologies of the Cu_6Sn_5 phase in tin-based Babbitt alloy (**a**) without the addition of nanoparticles; (**b**) 0.5 wt% iron oxide nanoparticles; (**c**) 0.5 wt% silica nanoparticles; (**d**) 0.25 wt% iron oxide and 0.25 wt% silica nanoparticles [102].

4.2. Nanocomposites in the Interlayer of Bimetallic Materials

In one study, bimetallic steel/aluminum composites containing strong interfacial bonding were prepared [103], wherein a continuous and uniform interfacial layer was developed during the tinning process. An additional preheat treatment on the steel substrate and a tinning process were applied. A super bonding strength of ~32 MPa for Al_2O_3 steel/aluminum bimetal castings was noted when using a nanoparticle-reinforced tin interlayer. It was reported that a low Al_2O_3 nanoparticle loading of 0.25 wt% and a steel substrate preheat treatment were suggested for better interfacial layer in steel/aluminum upholding the alloy bimetallic composite material.

To support and control the rotating or sliding motion of the mechanical parts, the bearings hold a special place in the industry. The selection of bimetallic bearing materials and their fabrication techniques should be carefully chosen while aiming for achieving the compressive strength, wear, fatigue, and corrosion resistance characteristics of bearings. Generally, bearing materials are grouped into the following three main categories: (a) white metals (tin-based and lead-based alloys, Babbitt); (b) copper–tin–lead alloys; and (c) aluminum–tin–lead alloys.

Improving the quality and performance of bimetallic bearing materials has become crucial for automotive and other related engineering applications. The performance of bearings is determined by the material design of the working layer, as well as the fabrication techniques. Tin-based alloys (Babbitt) are considered better materials for sliding bearings, such as for journal and thrust bearing applications. In fact, with the available technologies for the fabrication of bearings, traditional composites have reached an optimum to their mechanical properties and a fresh approach is desired to improve their existing performance.

This review presented and analyzed the importance of adding nanomaterials to the working surface layer, as well as the interlayer, of bimetallic materials fabricated by bimetal casting, in addition to encouraging researchers to design, develop and adopt novel strate-

gies using bimetal casting routes for metal and nanoparticle reinforcements in bearing materials for heavy-duty and high-load carrying capacities. The metal and/or nanoparticles should be selected and loaded carefully to improve the bearing material's performance without affecting that of the metallic shaft. Research should focus on the effects of the added metal and ceramic nanoparticles on the structures of the bearing materials, as well as the effects of the processing parameters on the structure, wear and mechanical properties, to develop novel nanocomposite bimetallic bearings for use in a wide range of bearing materials.

5. Conclusions

The outstanding properties of metal matrix nanocomposite castings direct the materials science community to develop advanced castings for next-generation engineering applications that demand products with enhanced properties while simultaneously being more economical and lower in weight. In this work, developments and new trends in metal matrix nanocomposite castings are reported with special attention paid to past and present manufacturing routes and schemes. The advantages and limitations of the nanocomposite castings are highlighted for both ferrous and nonferrous metal matrix nanocomposites. The modifications to the existing processes in terms of nanotechnology and dispersion of nanoparticles in metallic matrices are discussed, as well as the evolution of the strengthening mechanisms due to the incorporation of nanoparticles into the metallic matrices. Lastly, future fabrication methods for the development of metal matrix nanocomposite castings in combination with nanotechnological approaches for the manufacturing of materials are presented for novel castings of metal matrix nanocomposites.

In the following points, future insights into the development of metal matrix nanocomposite castings are summarized:

- Upon surveying the published articles, especially on steel castings, it was observed that limited research exists regarding the fabrication process and the related properties of metal matrix nanocomposite castings, which possess very important properties for functional use in high-performance engineering applications together with excellent mechanical performance;
- Other manufacturing routes should be investigated, along with secondary treatments, to broaden the application scope of metal matrix nanocomposite castings. Processes such as hot/cold working, homogenization and heat treatment should be employed to alter the microstructure and create a novel scheme of dispersed and uniformed precipitates at the nanoscale in metal matrices;
- Careful assessments of the relationship between the nanoparticle dispersion, distribution in the metal casting matrix and the properties of the promising metal matrix nanocomposite castings are obligatory required;
- Nanocomposites in the working surface layer and interlayer of the bimetallic materials are presented and thoroughly discussed. Significant improvements in the surface microstructure and shear strength of the bimetallic bearing are achieved by the nanoparticles in addition to the surface working layer and interlayer areas.

In summary, there is still a huge undiscovered wealth in metal matrix nanocomposite castings that can be revealed with a careful combination of nanometer-sized particles along with cast metal matrices and, hence, multi-functionalities could be achieved in a single material.

Author Contributions: Conceptualization, M.R. and T.S.; methodology, T.S.; validation, A.K., N.F. and K.S.A.H.; formal analysis, N.F.; investigation, A.K.; resources, K.S.A.H.; data curation, M.R.; writing—original draft preparation, M.R.; writing—review and editing, T.S.; visualization, N.F.;

supervision, M.R.; project administration, T.S.; funding acquisition, M.R. All authors have read and agreed to the published version of the manuscript.

Funding: This research has been funded by Scientific Research Deanship at University of Ha'il-Saudi Arabia, through project number: <<RG-23 185>>.

Data Availability Statement: No new data were created or analyzed in this study.

Acknowledgments: Thanks to the above funds.

Conflicts of Interest: The authors declare no conflicts of interest.

References

1. Kalpakjian, S.; Schmid, S. *Manufacturing Engineering & Technology*, 7th ed.; Pearson: London, UK, 2013.
2. Colás, R.; Rodríguez, A.; Talamantes, J.; Valtierra, S. Solidification analysis of aluminium engine block. *Int. J. Cast Met. Res.* **2004**, *17*, 332–338. [CrossRef]
3. American Foundry Society. About Metalcasting. 2020. Available online: https://www.afsinc.org/about-metalcasting (accessed on 21 November 2024).
4. Yadav, V. Nanotechnology, Big things from a Tiny World: A Review, Advance in Electronic and Electric Engineering. *Int. J. u-e-Serv. Sci. Technol.* **2013**, *3*, 771–778.
5. Stirling, D.A. *The Nanotechnology Revolution: A Global Bibliographic Perspective*; CRC Press: Boca Raton, FL, USA, 2018.
6. Goddard, W.A., III; Brenner, D.; Lyshevski, S.E.; Iafrate, G.J. *Handbook of Nanoscience, Engineering, and Technology*, 3rd ed.; CRC Press: Boca Raton, FL, USA, 2012.
7. Ibrahim, I.; Mohamed, F.; Lavernia, E. Particulate reinforced metal matrix composites—A review. *J. Mater. Sci.* **1991**, *26*, 1137–1156. [CrossRef]
8. Kim, Y.; Lee, J.; Yeom, M.S.; Shin, J.W.; Kim, H.; Cui, Y.; Kysar, J.W.; Hone, J.; Jung, Y.; Jeon, S.; et al. Strengthening effect of single-atomic-layer graphene in metal–graphene nanolayered composites. *Nat. Commun.* **2013**, *4*, 2114. [CrossRef]
9. Mishra, R.R.; Panda, A.; Sahoo, A.K.; Kumar, R. Characterization and machinability analysis of aluminium-based metal matrix composites (MMC): A critical review. *Proc. Inst. Mech. Eng. Part C J. Mech. Eng. Sci.* **2025**, *239*, 861–884. [CrossRef]
10. Polayya, C.; Rao, C.S.; GB, V.K. Enhancing tribological and corrosion characteristics of AA2099/GNP metal matrix nanocomposites through parametric optimization using Taguchi Technique. *Mater. Res. Express* **2025**, *12*, 015009. [CrossRef]
11. Kmita, A.; Dańko, R.; Holtzer, M.; Hutera, B.; Stypuła, B. Utilisation of nanoparticles in technologies of producing castings for the needs of power engineering. *Nanomater. Energy* **2014**, *3*, 53–60. [CrossRef]
12. Bawane, K.; Lu, K. Microstructure evolution of nanostructured ferritic alloy with and without Cr_3C_2 coated SiC at high temperatures. *J. Mater. Sci. Technol.* **2020**, *43*, 126–134. [CrossRef]
13. Jiang, S.H.; Wang, H.; Wu, Y.; Liu, X.; Chen, H.; Yao, M.; Gault, B.; Ponge, D.; Raabe, D.; Hirata, A.; et al. Ultrastrong steel via minimal lattice misfit and high-density nanoprecipitation. *Nature* **2017**, *544*, 460–464. [CrossRef]
14. Rodríguez, E.; Pérez, A.; Mercado-Solis, R.D.; Abraham, V.-T.; Jiménez, O.; Flores, M.; González, M.A.; Ibarra, J. Erosion problem in tool steel using cold box core-making process. *China Foundry* **2019**, *16*, 204–210. [CrossRef]
15. Han, X.; Zhang, Z.P.; Hou, J.Y.; Barber, G.C.; Qiu, F. Tribological behavior of shot peened/austempered AISI 5160 steel. *Tribol. Int.* **2020**, *145*, 106197. [CrossRef]
16. Li, H.-C.; Liu, Y.-X.; Zhang, Y.-H.; Liu, Z.; Zhai, Q.-J. Effects of hot top pulsed magneto-oscillation on solidification structure of steel ingot. *China Foundry* **2018**, *15*, 110–116. [CrossRef]
17. Hao, L.; Ji, X.; Zhang, G.; Zhao, W.; Sun, M.; Peng, Y. Carbide precipitation behavior and Mechanical properties of micro-alloyed medium Mn steel. *J. Mater. Sci. Technol.* **2020**, *47*, 122–130. [CrossRef]
18. Zhang, H.J.; Li, C.; Guo, Q.Y.; Ma, Z.; Li, H.; Liu, Y. Improving creep resistance of nickel-based superalloy Inconel 718 by tailoring gamma double prime variants. *Scr. Mater.* **2019**, *164*, 66–70. [CrossRef]
19. Zhang, K. Design of real time monitor system of manufacture process of iron and steel industry based on new style sensors. *Energy Procedia* **2012**, *16*, 627–632. [CrossRef]
20. Melchers, R.E. Long-term corrosion of cast irons and steel in marine and atmospheric environments. *Corros. Sci.* **2013**, *68*, 186–194. [CrossRef]
21. Chen, B.; Yang, J.-X.; Ouyang, Z.-Y. Life cycle assessment of internal recycling options of steel slag in Chinese iron and steel industry. *J. Iron Steel Res. Int.* **2011**, *18*, 33–40. [CrossRef]
22. Kalpakjian, S.; Schmid, S.R. *Manufacturing Engineering and Technology*, 6th ed.; Pearson Education, Inc.: London, UK, 2010; p. 239.
23. Qiu, F.; Liu, T.-S.; Zhang, X.; Chang, F.; Shu, S.-L.; Yang, H.-Y.; Zhao, Q.-L.; Jiang, Q.-C. Application of nanoparticles in cast steel: An overview. *China Foundry* **2020**, *17*, 111–126. [CrossRef]

24. Pan, N.; Song, B.; Zhai, Q.J.; Wen, B. Effect of lattice disregistry on the heterogeneous nucleation catalysis of liquid steel. *J. Univ. Sci. Technol.* **2011**, *32*, 179–190.
25. Dong, B.X.; Yang, H.Y.; Qiu, F.; Li, Q.; Shu, S.L.; Zhang, B.Q.; Jiang, Q.C. Design of TiCx nanoparticles and their morphology manipulating mechanisms by stoichiometric ratios: Experiment and first-principle calculation. *Mater. Des.* **2019**, *181*, 107951. [CrossRef]
26. Ohashi, T.; Fujii, H.; Nuri, Y.; Asano, K. Effect of oxides on nucleation behavior in supercooled iron. *Trans. Iron Steel Inst. Jpn.* **1977**, *17*, 262. [CrossRef]
27. Bramfitt, B. The effect of carbide and nitride additions on the heterogeneous nucleation behavior of liquid iron. *Metall. Trans.* **1970**, *1*, 1987. [CrossRef]
28. Suzuki, T.; Inoue, J.; Koseki, T. Solidification of iron and steel on single-crystal oxide. *ISIJ Int.* **2007**, *47*, 847–852. [CrossRef]
29. He, B.; Tian, H.; Yu, G.; Shi, Z. A Review of Composite Gears. *Mech. Compos. Mater.* **2025**, *60*, 1133–1154. [CrossRef]
30. Lei, Y.; Liu, Z.Y.; Li, H. Study on super-fine grains obtained in low carbon section steels by adding ZrC. *Iron Steel* **2002**, *37*, 58–60.
31. Lei, Y.; Liu, Z.Y.; Li, H. Study on super-fine grain obtained in low-carbon section steels by adding ZrO_2. *Ordnance Mater. Sci. Eng.* **2004**, *27*, 3–5.
32. Wang, G.C.; Wang, T.M.; Li, S.N. Study on the process of adding Al_2O_3 nano-powder to molten pure iron. *J. Univ. Sci. Technol.* **2007**, *29*, 579–581.
33. Wang, G.C.; Fang, K.M.; Wang, T.M. Study on super-fine particle of TiN added into molten pure iron. *Iron Steel Vanadium Titan.* **2006**, *27*, 21–25.
34. Li, X.L.; Wang, J.M.; He, C.L. Effect of nano-SiC particles addition on microstructure and hardness of Q235 Steel. *Foundry* **2009**, *58*, 229–231.
35. Lazarova, R.; Petrov, R.; Gaydarova, V.; Davidkov, A.; Alexeev, A.; Manchev, M.; Manolov, V. Microstructure and mechanical properties of P265GH cast steel after modification with TiCN particles. *Mater. Des.* **2011**, *32*, 2734–2741. [CrossRef]
36. Xiao, F.R.; Liao, B. Refinement effectiveness of self-prepared (NbTi) C nanoparticles on as-cast 1045 steel. *J. Mater. Des.* **2018**, *139*, 531–540.
37. Yang, K.; Liang, Y.; Yan, W.; Shan, Y. Preferential distribution of boron and its effect on microstructure and mechanical properties of (9–12)%Cr martensitic heat resistant steels. *Acta Metall. Sin.* **2020**, *56*, 53–65.
38. Wu, X.; Zuo, X.R.; Zhao, W.W. Mechanism of TiN fracture during the tensile process of NM500 wear-resistant steel. *Acta Metall. Sin.* **2020**, *56*, 129–136.
39. Yu, W.X.; Liu, B.X.; He, J.N.; Chen, C.X.; Fang, W.; Yin, F.X. Microstructure characteristics, strengthening and toughening mechanism of rolled and aged multilayer TWIP/maraging steels. *Mater. Sci. Eng. A* **2019**, *767*, 138426. [CrossRef]
40. Xu, L.; Wei, D.-Y.; Yu, Y.; Zhang, H.; Bai, B.-Z. Effect of microstructure on corrosion fatigue behavior of 1500 MPa level carbide-free bainite/martensite dual-phase high strength steel. *J. Iron Steel Res. Int.* **2011**, *18*, 63–67. [CrossRef]
41. Mao, C.L.; Liu, C.X.; Yu, L.M.; Li, H.; Liu, Y. The correlation among microstructural parameter and dynamic strain aging (DSA) in influencing the mechanical properties of a reduced activated ferritic-martensitic (RAFM) steel. *Mater. Sci. Eng. A* **2019**, *739*, 90–98. [CrossRef]
42. Shi, R.J.; Wang, Z.D.; Qiao, L.J.; Pang, X. Microstructure evolution of insitu nanoparticles and its comprehensive effect on high strength steel. *J. Mater. Sci. Technol.* **2019**, *35*, 1940–1950. [CrossRef]
43. Chen, Y.; Hong, Z.; Zhang, X.; Xia, M.; Yan, Q.; Ge, C. Enhanced creep resistance of Y-bearing 9Cr ferritic/martensitic steel via vacuum casting technique. *J. Mater. Res. Technol.* **2019**, *8*, 4588–4597. [CrossRef]
44. Yang, C.Y.; Luan, Y.K.; Li, D.Z.; Li, Y. Effects of rare earth elements on inclusions and impact toughness of high-carbon chromium bearing steel. *J. Mater. Sci. Technol.* **2020**, *35*, 1298–1308. [CrossRef]
45. Dai, L.; Liu, Z.; Yu, L.; Liu, Y.; Shi, Z. Microstructural characterization of Mg-Al-O rich nanophase strengthened Fe-Cr alloys. *Mater. Sci. Eng. A* **2020**, *777*, 138664. [CrossRef]
46. Zhao, Q.; Yu, L.; Liu, Y.; Huang, Y.; Ma, Z.; Li, H.; Wu, J. Microstructure and tensile properties of a 14Cr ODS ferritic steel. *Mater. Sci. Eng. A* **2017**, *680*, 347–350. [CrossRef]
47. Dou, P.; Sang, W.; Kimura, A. Morphology, crystal and metal/oxide interface structures of nanoparticles in Fe_{15}Cr-2W-0.5Ti-7Al-0.4Zr-0.5Y_2O_3 ODS steel. *J. Nucl. Mater.* **2019**, *523*, 231–247. [CrossRef]
48. Alharbi, A.; Khan, A.; Todd, I.; Ramadan, M.; Mumtaz, K. Semisolid heat treatment processing window of Pb-40% Sn alloy for feedstock in the 3D printing thixo-forming process. *Mater. Today Proc.* **2021**, *51*, 403–410. [CrossRef]
49. Todaro, C.J.; Easton, M.A.; Qiu, D.; Zhang, D.; Bermingham, M.J.; Lui, E.W.; Brandt, M.; StJohn, D.H.; Qian, M. Grain structure control during metal 3D printing by high-intensity ultrasound. *Nat. Commun.* **2020**, *11*, 142. [CrossRef]
50. Yu, C.; Zhang, P.; Zhang, Z.; Liu, W. Microstructure and fatigue behavior of laser-powder bed fusion austenitic stainless steel. *J. Mater. Sci. Technol.* **2020**, *46*, 191–200. [CrossRef]
51. Tan, C.L.; Zhou, K.S.; Ma, W.Y.; Zeng, D. Research progress of laser additive manufacturing of maraging steels. *Acta Metall. Sin.* **2020**, *56*, 36–52.

52. Wang, L.; Xing, H.; Li, Y.; Wang, J. Toward multiscale simulations for solidification microstructure and microsegregation for selective laser melting of nickel-based superalloys. *J. Mater. Res. Technol.* **2023**, *25*, 3574–3587. [CrossRef]
53. Dadbakhsh, S.; Mertens, R.; Hao, L.; van Humbeeck, J.; Kruth, J.P. Selective laser melting to manufacture "in situ" metal matrix composites: A review. *Adv. Eng. Mater.* **2019**, *21*, 1801244. [CrossRef]
54. Mussatto, A.; Groarke, R.; A-Hameed, A.; Ahad, I.U.; Vijayaraghavan, R.K.; O'Neill, A.; McNally, P.; Delaure, Y.; Brabazon, D. Evaluation via powder metallurgy of nano-reinforced iron powders developed for selective laser melting applications. *Mater. Des.* **2019**, *182*, 108046. [CrossRef]
55. Gilliard, M.B.; Pierini, B.T.; Alconchel, S.A. In situ formation of Fe–NbC/C composite powders from solution-derived precursors by a gas reduction-carburization process. *Ceram. Int.* **2014**, *40*, 14881–14889. [CrossRef]
56. Huang, X.; Qi, X.; Boey, F.; Zhang, H. Graphene-based composites. *Chem. Soc. Rev.* **2012**, *41*, 666–686. [CrossRef] [PubMed]
57. Riedel, R. Nanoscaled inorganic materials by molecular design. *Chem. Soc. Rev.* **2012**, *41*, 5029–5031. [CrossRef] [PubMed]
58. Ammisetti, D.K.; Sai Sarath, K.; Harish Kruthiventi, S.S. A Review on Mechanical and Wear Characteristics of Magnesium Metal Matrix Composites. *J. Tribol.* **2025**, *147*, 020801. [CrossRef]
59. Dieringa, H. Properties of magnesium alloys reinforced with nanoparticles and carbon nanotubes: A review. *J. Mater. Sci.* **2011**, *46*, 289–306. [CrossRef]
60. Bang, J.H.; Suslick, K.S. Applications of ultrasound to the synthesis of nanostructured materials. *Adv. Mater.* **2010**, *22*, 1039–1059. [CrossRef]
61. Abdullah, A.; Pak, A.; Abdullah, M.M.; Shahidi, A.; Malaki, M. Study of the behavior of ultrasonic piezo-ceramic actuators by simulations. *Electron. Mater. Lett.* **2014**, *10*, 37–42. [CrossRef]
62. Hamedan, A.D.; Shahmiri, M. Production of A356–1 wt% SiC nanocomposite by the modified stir casting method. *Mater. Sci. Eng. A* **2012**, *556*, 921–926. [CrossRef]
63. Sajjadi, S.; Ezatpour, H.; Beygi, H. Microstructure and mechanical properties of Al–Al_2O_3 micro and nano composites fabricated by stir casting. *Mater. Sci. Eng. A* **2011**, *528*, 8765–8771. [CrossRef]
64. Suresh, S.; Mishra, D.; Srinivasan, A.; Arunachalam, R.; Sasikumar, R. Production and characterization of micro and nano Al_2O_3 particle-reinforced LM25 aluminium alloy composites. *ARPN J. Eng. Appl. Sci.* **2011**, *6*, 94–98.
65. Akbari, M.K.; Mirzaee, O.; Baharvandi, H. Fabrication and study on mechanical properties and fracture behavior of nanometric Al_2O_3 particle-reinforced A356 composites focusing on the parameters of vortex method. *Mater. Des.* **2013**, *46*, 199–205. [CrossRef]
66. Gupta, M.; Ling, S.N.M. *Magnesium, Magnesium Alloys, and Magnesium Composites*; John Wiley & Sons: Hoboken, NJ, USA, 2011.
67. Alam, M.T.; Arif, S.; Ansari, A.H. Mechanical Behaviour and Morphology of A356/SiC Nanocomposites Using Stir Casting. In *IOP Conference Series: Materials Science and Engineering*; IOP Publishing: Bristol, UK, 2017; p. 012293.
68. Khandelwal, A.; Mani, K.; Srivastava, N.; Gupta, R.; Chaudhari, G. Mechanical behavior of AZ31/Al_2O_3 magnesium alloy nanocomposites prepared using ultrasound assisted stir casting. Compos. *Part B Eng.* **2017**, *123*, 64–73. [CrossRef]
69. Srivatsan, T.; Godbole, C.; Paramsothy, M.; Gupta, M. Influence of nano-sized carbon nanotube reinforcements on tensile deformation, cyclic fatigue, and final fracture behavior of a magnesium alloy. *J. Mater. Sci.* **2012**, *47*, 3621–3638. [CrossRef]
70. Gupta, M.; Wong, W. Magnesium-based nanocomposites: Lightweight materials of the future. *Mater. Charact.* **2015**, *105*, 30–46. [CrossRef]
71. De Cicco, M.P.; Li, X.; Turng, L.-S. Semi-solid casting (SSC) of zinc alloy nanocomposites. *J. Mater. Process Technol.* **2009**, *209*, 5881–5885. [CrossRef]
72. Cravotto, G.; Gaudino, E.C.; Cintas, P. On the mechanochemical activation by ultrasound. *Chem. Soc. Rev.* **2013**, *42*, 7521–7534. [CrossRef]
73. Xu, H.; Zeiger, B.W.; Suslick, K.S. Sonochemical synthesis of nanomaterials. *Chem. Soc. Rev.* **2013**, *42*, 2555–2567. [CrossRef]
74. Ma, C.; Chen, L.; Cao, C.; Li, X. Nanoparticle-induced unusual melting and solidification behaviours of metals. *Nat. Commun.* **2017**, *8*, 14178. [CrossRef]
75. Baig, R.N.; Varma, R.S. Alternative energy input: Mechanochemical, microwave and ultrasound-assisted organic synthesis. *Chem. Soc. Rev.* **2012**, *41*, 1559–1584. [CrossRef]
76. Xu, W.; Tzanakis, I.; Srirangam, P.; Mirihanage, W.; Eskin, D.; Bodey, A.; Lee, P. Synchrotron quantification of ultrasound cavitation and bubble dynamics in Al–10Cu melts. *Ultrason. Sonochem.* **2016**, *31*, 355–361. [CrossRef]
77. Dieringa, H. Processing of Magnesium-Based Metal Matrix Nanocomposites by Ultrasound-Assisted Particle Dispersion: A Review. *Metals* **2018**, *8*, 431. [CrossRef]
78. Kudryashova, O.; Vorozhtsov, S. On the Mechanism of Ultrasound-Driven Deagglomeration of Nanoparticle Agglomerates in Aluminum Melt. *JOM* **2016**, *68*, 1307–1311. [CrossRef]
79. Malaki, M.; Xu, W.; Kasar, A.K.; Menezes, P.L.; Dieringa, H.; Varma, R.S.; Gupta, M. Advanced Metal Matrix Nanocomposites. *Metals* **2019**, *9*, 330. [CrossRef]
80. Alghamdi, A.S.; Ramadan, M.; Halim, K.S.A.; Fathy, N. Microscopical Characterization of Cast Hypereutectic Al-Si Alloys Reinforced with Graphene Nanosheets. *Eng. Technol. Appl. Sci. Res.* **2018**, *8*, 2514–2519. [CrossRef]

81. Ramadan, M.; Fathy, N.; Abdel Halim, K.S.; Alghamdi, A.S. New trends and advances in bimetal casting technologies. *Int. J. Adv. Appl. Sci.* **2019**, *6*, 75–80.
82. Ramadan, M.; Alghamdi, A.S. Interfacial microstructures and properties of hyper-eutectic Al–21Si/hypo-eutectic Al–7.5Si bimetallic material fabricated by liquid–liquid casting route. *Mech. Sci.* **2020**, *11*, 371–379. [CrossRef]
83. Fathy, N.; Ramadan, M.; Hafez, K.M.; Abdulaziz, F.; Ayadi, B.; Alghamdi, A.S. A Novel Approach of Optimum Time Interval Estimation for Al-7.5Si/Al-18Si Liquid–Liquid Bimetal Casting in Sand and Metallic Moulds. *Materials* **2023**, *16*, 3004. [CrossRef]
84. Tavakoli, A.M.; Nami, B.; Malekan, M.; Khoubrou, I. Influences of Coating Type on Microstructure and Strength of Aluminum–Steel Bimetal Composite Interface. *Int. J. Met.* **2022**, *16*, 689–698. [CrossRef]
85. Suryadarma, E.H.E.; Ai, T.J.; Bawono, B.; Siswantoro, A.T. Improving Bimetal Bond Quality Between Cast Steel and Aluminum Alloys Using Response Surface Methodology. *Int. J. Met.* **2022**, *16*, 1432–1441. [CrossRef]
86. Ramadan, M.; Alghamdi, A.S.; Subhani, T.; Halim, K.S.A. Fabrication and Characterization of Sn-Based Babbitt Alloy Nanocomposite Reinforced with Al_2O_3 Nanoparticles/Carbon Steel Bimetallic Material. *Materials* **2020**, *13*, 2759. [CrossRef]
87. Jiang, W.; Fan, Z.; Li, G.; Yang, L.; Liu, X. Effects of Melt-to-Solid Insert Volume Ratio on the Microstructures and Mechanical Properties of Al/Mg Bimetallic Castings Produced by Lost Foam Casting. *Met. Mater. Trans. A* **2016**, *47*, 6487–6497. [CrossRef]
88. Jiang, W.; Jiang, Z.; Li, G.; Wu, Y.; Fan, Z. Microstructure of Al/Al bimetallic composites by lost foam casting with Zn interlayer. *Mater. Sci. Technol.* **2017**, *34*, 487–492. [CrossRef]
89. Shangguan, J.; Zhao, J.; Shi, Y.; Gu, C.; Jin, B.; Cheng, J.; Guo, Y. Effects of Zn Interlayer on Microstructures and Mechanical Properties of TC4/AZ91D Bimetal via Solid–Liquid Compound Casting Process. *Int. J. Met.* **2022**, *16*, 419–434. [CrossRef]
90. Guan, F.; Fan, S.; Wang, J.; Li, G.; Zhang, Z.; Jiang, W. Effect of Vibration Acceleration on Interface Microstructure and Bonding Strength of Mg–Al Bimetal Produced by Compound Casting. *Metals* **2022**, *12*, 766. [CrossRef]
91. Cholewa, M.; Wróbel, T.; Tenerowicz, S. Bimetallic layer castings. *J. Achiev. Mater. Manuf. Eng.* **2010**, *43*, 385–391.
92. Wrobel, T. Characterization of Bimetallic Castings with an Austenitic Working Surface Layer and an Unalloyed Cast Steel Base. *J. Mater. Eng. Perform.* **2014**, *23*, 1711–1717. [CrossRef]
93. Jiang, W.; Fan, Z.; Li, C. Improved steel/aluminum bonding in bimetallic castings by a compound casting process. *J. Mater. Process. Technol.* **2015**, *226*, 25–31. [CrossRef]
94. Jiang, W.; Fan, Z.; Li, G.; Liu, X.; Liu, F. Effects of hot-dip galvanizing and aluminizing on interfacial microstructures and mechanical properties of aluminum/iron bimetallic composites. *J. Alloys Compd.* **2016**, *688*, 742–751. [CrossRef]
95. Li, G.; Yang, W.; Jiang, W.; Guan, F.; Jiang, H.; Wu, Y.; Fan, Z. The Role of Vacuum Degree in the Bonding of Al/Mg Bimetal Prepared by a Compound Casting Process. *J. Mech. Work. Technol.* **2019**, *265*, 112–121. [CrossRef]
96. Ramadan, M.; Alghamdi, A.S.; Hafez, K.M.; Subhani, T.; Halim, K.S.A. Development and Optimization of Tin/Flux Mixture for Direct Tinning and Interfacial Bonding in Aluminum/Steel Bimetallic Compound Casting. *Materials* **2020**, *13*, 5642. [CrossRef]
97. Cholewa, M.; Tenerowicz, S.; Wróbel, T. Quality of the joint between cast steel and cast iron in bimetallic castings. *Arch. Foundry Eng.* **2008**, *3*, 37–40.
98. Ramadan, M. Interface Structure and Elements Diffusion of As-Cast and Annealed Ductile Iron/Stainless Steel Bimetal Castings. *Eng. Technol. Appl. Sci. Res.* **2018**, *8*, 2709–2714. [CrossRef]
99. Ramadan, M.; Hafez, K.M.; Alghamdi, A.S.; Ayadi, B.; Abdel Halim, K.S. Novel Approach for Using Ductile Iron as Substrate in Bimetallic Materials for Higher Interfacial Bonding Bearings. *Int. J. Met.* **2022**, *16*, 987–1000. [CrossRef]
100. Ramadan, M.; Hafez, K. Interfacial microstructure and hardness of Sn-Based Babbitt/C93700 Cu-Pb-Sn bimetallic materials. *Mater. Today Proc.* **2021**, *45*, 5074–5080. [CrossRef]
101. Babu, M.V.S.; Krishna, A.R.; Suman, K. Improvement of Tensile Behaviour of Tin Babbitt by Reinforcing with Nano Ilmenite and its Optimisation by using Response Surface Methodology. *Int. J. Manuf. Mater. Mech. Eng.* **2017**, *7*, 37–51. [CrossRef]
102. Ramadan, M.; Subhani, T.; Hafez, K.M.; Fathy, N.; Ayadi, B.; Abdel Halim, K.S.; Alghamdi, A.S.; Ibrahim, K.M. Microstructure and Mechanical Performance of Tin-Based Babbitt Alloy Containing Iron Oxide and Silica Nanoparticles. *Metals* **2023**, *13*, 324. [CrossRef]
103. Ramadan, M.; Khaliq, A.; Hafez, K.M.; Alghamdi, A.S.; Fathy, N.; Harraz, F.A.; Ayadi, B.; Abdel Halim, K.S. Super Bonding Strength of Al_2O_3 Nanoparticles Reinforced Sn Interlayer Steel/Aluminum Bimetal Casting. *Crystals* **2022**, *12*, 324. [CrossRef]

Disclaimer/Publisher's Note: The statements, opinions and data contained in all publications are solely those of the individual author(s) and contributor(s) and not of MDPI and/or the editor(s). MDPI and/or the editor(s) disclaim responsibility for any injury to people or property resulting from any ideas, methods, instructions or products referred to in the content.